TOROIDAL PATH FILTER

Salvatore Alfano*

For satellite conjunction prediction containing many objects, timely processing can be a concern. Various filters are used to identify orbiting pairs that cannot come close enough over a prescribed time period to be considered hazardous. Such pairings can then be eliminated from further computation to quicken the overall processing time. One such filter is the orbit path filter (also known as the geometric pre-filter), designed to eliminate pairs of objects based on characteristics of orbital motion. The goal of this filter is to eliminate pairings where the distance (geometry) between their orbits remains above some user-defined threshold, irrespective of the actual locations of the satellites along their paths. Rather than using a single distance bound, this work presents a toroid approach, providing a measure of versatility by allowing the user to specify different in-plane and out-of-plane bounds for the path filter. The primary orbit is used to define a focus-centered elliptical ring torus with user-defined thresholds. An assessment is then made to determine if the secondary orbit can touch or penetrate this torus. The method detailed here can be used on coplanar, as well as non-coplanar, orbits.

INTRODUCTION

As the number of orbiting satellites and space debris grows, so does the concern of possible collision. Predicting future close encounters is becoming a routine requirement. In 2004, as a free service to the satellite operator community, the Center for Space Standards & Innovation (CSSI) began offering SOCRATES[1]—Satellite Orbital Conjunction Reports Assessing Threatening Encounters in Space. Twice each day, limited only by data availability, CSSI runs a list of all satellite payloads on orbit against a list of all objects on orbit using the catalog of all unclassified NORAD two-line element sets (TLEs) to predict conjunctions within 5 kilometers over the next seven days. As of June 6, 2011, SOCRATES regularly processes 14,435 tracks in earth orbit, of which 3,078 are designated as payloads or primary objects. While not all of these payloads are still active, about a third of them are and they perform a variety of important tasks, many vital to the global economy. For the purposes of this work, a conjunction is defined as a point in time when the relative range rate is zero and the range is below the desired threshold.

For the all-on-all conjunction problem the set of primary objects contain all of the secondary objects. When dealing with such large numbers of space objects and pairings, timely processing becomes a concern. Conjunction filters provide an efficient mechanism for eliminating further analysis by providing quick identification of primary/secondary pairings which cannot come close enough over the time interval to yield a conjunction. Because each pairing of objects must be considered independently, the assessment of the entire catalog lends itself well to parallelization as detailed by Coppola et al[2]. As they pointed out, software performance can by markedly improved by foregoing direct search methods on each and every pairing in favor of more selective algorithms which can quickly eliminate pairs of objects based on characteristics of orbital motion. They accomplish this through a series of geometrical and temporal filters to quickly reduce the search space.

* Senior Research Astrodynamicist, Center for Space Standards and Innovation (CSSI), 7150 Campus Drive, Suite 260, Colorado Springs, CO, 80920-6522, salfano@centerforspace.com, AIAA Associate Fellow.

Hoots et al[3] described a series of three screening filters through which candidate pairings should pass before determining their close approach distance. Two of the filters are geometrical and one uses the known properties of the orbital motion of the two objects. These filters serve to screen each pairing of objects in the catalogue, eliminating many of those from further scrutiny and thus greatly reducing the number of computations needed. After the screening, the trajectories of the remaining candidate objects are sampled to determine the actual close approach periods. The three filters are referred to as the Apogee/Perigee filter, the orbit path filter (also known as the geometric pre-filter) and the time filter. Woodburn et al[4] examined these filters and subsequently discovered occasional inadequacies when implemented as originally described. The work presented in this article concerns itself only with the orbit path filter.

The goal of the orbit path filter is to eliminate pairings which cannot produce conjunctions because the distance (geometry) between their orbits remains above some user-defined threshold, irrespective of the actual locations of the satellites along their paths. Woodburn's team stated that such filters define a proxy for the distance between a candidate conjunction pair and then either eliminate the pair from further consideration or limit the time periods requiring further analysis. They further explained that such filters use approximations based on known characteristics of orbital motion to maximize the efficiency of the computation. Care must be taken that the accuracy of the results not be compromised by these approximations. One simple method of accounting for approximations is to use distance pads to increase the size of the conjunction threshold distance during the filtering process. Such padding increases the number of candidate pairs passing through each filter in order to reduce the likelihood that those pairs will be improperly eliminated which could lead to a missed conjunction.

Rather than use an orbit path filter that assesses the minimum conjunction threshold distance between two orbit trajectories, this work employs a torus with differing in-plane and out-of-plane tube boundaries to give the user more versatility. The primary orbit's instantaneous, Keplerian, mean elements are used to define a focus-centered elliptical ring torus with user-defined thresholds. An assessment is then made to determine if the secondary orbit can touch or penetrate this torus. If it cannot, then this pair can be eliminated from further consideration.

FUNDAMENTAL TORUS EQUATIONS

This section shows how to modify the standard torus equation to accommodate an elliptical orbit with different radial and out-of-plane tube boundaries. All surface points (*x, y, z*) of a ring torus radially symmetric about the z-axis must satisfiy

$$\left(R - \sqrt{x^2 + y^2}\right)^2 + z^2 = r^2 \tag{1}$$

where R is the radial distance from the center of the torus to the center of the tube, and r is the circular radius of the tube as shown in Figure 1.
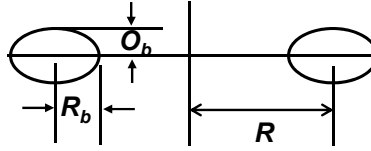
Full View   Cross Section
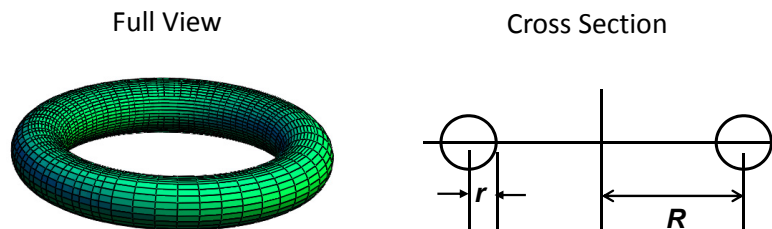
For an elliptical cross section the tube surface points can be expressed by

$$\frac{\left(R - \sqrt{x^2 + y^2}\right)^2}{\left(R_b\right)^2} + \frac{z^2}{\left(O_b\right)^2} = 1 \tag{2}$$

where R_b is the in-plane (radial) axis boundary and O_b is the out-of-plane axis boundary as shown in Figure 2.

Cross Section

Figure 2. Cross section of elliptical tube.

The radial distance from the center of the torus to the center of the tube can be represented as an ellipse by modifying R. As a function of an orbit's true anomaly ν, eccentricity ecc, and semi-major axis a, the torus radius becomes

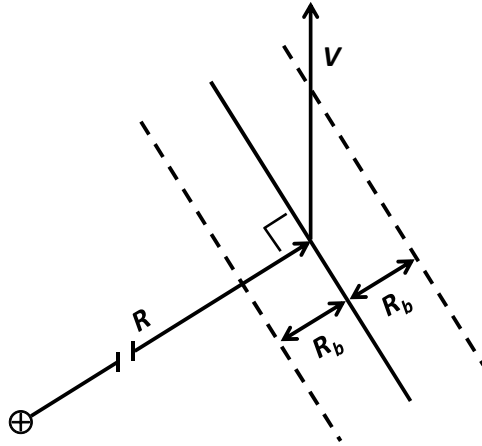$$R = \frac{a \cdot \left(1 - ecc^2\right)}{1 + ecc \cdot \cos(\nu)} \tag{3}$$

By aligning the x and y axes with P and Q in the perifocal coordinate frame, the cosine of true anomaly becomes

$$\cos(\nu) = \frac{x}{\sqrt{x^2 + y^2}} \tag{4}$$

These can now be substituted into Equation 2 to produce

$$\frac{\left[a \cdot \left(ecc^2 - 1\right) + \sqrt{x^2 + y^2} + ecc \cdot x\right]^2}{\left(\sqrt{x^2 + y^2} + ecc \cdot x\right)^2} \cdot \frac{\left(x^2 + y^2\right)}{\left(R_b\right)^2} + \frac{z^2}{\left(O_b\right)^2} = 1 \tag{5}$$

The in-plane axis boundary R_b is measured along the radius vector direction as shown in Figure 3.

Figure 3. In-plane axis representation of R_b.

For noncircular orbits, the velocity vector will only be perpendicular to the radius vector at perigee and apogee. If one desires to define the in-plane boundary V_b with respect to the in-track (velocity) direction, then Equation 5 must be modified in accordance with Figure 4 by assuming $R \gg V_b$.
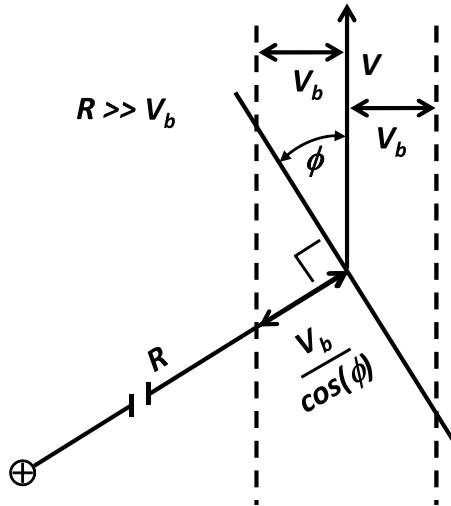
Figure 4. In-plane axis representation of V_b.

where ϕ is the in-plane flight path angle measured from the local horizon to the velocity vector. From simple orbital dynamics we know that the magnitude of the angular momentum h is related to orbital radius R, velocity V, and flight path angle ϕ through

$$h = R \cdot V \cdot cos(\phi) \tag{6}$$

Angular momentum can also be found through

$$h^2 = a \cdot \left(1 - ecc^2\right) \cdot \mu \tag{7}$$

4

where μ is the gravitational constant. V is simply

$$V = \sqrt{2 \cdot \left(\frac{-\mu}{2 \cdot a} + \frac{\mu}{R} \right)} \qquad (8)$$

Equations 6-8 can now be used to produce the expression

$$cos(\phi)^2 = \frac{a^2 \cdot \left(1 - ecc^2\right)}{R \cdot (2 \cdot a - R)} \qquad (9)$$

Equations 3 and 4 yield R in terms of x and y. Equation 5 can now be altered by substituting $V_b/cos(\phi)$ for R_b and expressing all in terms of *x, y, z*, and the constant orbital parameters *a* and *ecc*.

$$\frac{\left[a \cdot \left(ecc^2 - 1\right) + \sqrt{x^2 + y^2} + ecc \cdot x \right]^2}{\left(\sqrt{x^2 + y^2} + ecc \cdot x \right)^2 + ecc^2 \cdot y^2} \cdot \frac{\left(x^2 + y^2\right)}{\left(V_b\right)^2} + \frac{z^2}{\left(O_b\right)^2} = 1 \qquad (10)$$

When compared to Equation 5, the in-plane boundary V_b with respect to the in-track (velocity) direction causes an extra eccentricity-dependent term to appear in the denominator. For a circular orbit, eccentricity is zero, R_b and V_b are equivalent, and Equation 10 becomes identical to Equation 5.

Both equations completely define a focus-centered elliptical ring torus in the *x,y* plane bounded by O_b and R_b (or V_b). Equation 5 represents a radially-bounded elliptical tube over the torus path while Equation 10 represents an in-plane-bounded elliptical tube; both have an independent bound O_b for the out-of-plane axis. Given any position (*x, y, z*) and boundaries O_b and R_b (or V_b), one can immediately know if that position is inside, outside, or just touching the torus by simply determining if the left-hand side of Equation 5 (or 10) is less than one, greater than one, or equal to one respectively.

THE PERIFOCAL COORDINATE SYSTEM

As summarized by Xue and Li[5], for a Keplerian orbit with elements *a, ecc, inc*, Ω, and ω, the unit vectors of eccentricity (*P*), semi-latus rectum (*Q*), and orbital angular momentum (*W*) are defined as

$$P(\Omega, \omega, inc) = \begin{pmatrix} cos(\Omega) \cdot cos(\omega) - sin(\Omega) \cdot sin(\omega) \cdot cos(inc) \\ sin(\Omega) \cdot cos(\omega) + cos(\Omega) \cdot sin(\omega) \cdot cos(inc) \\ sin(\omega) \cdot sin(inc) \end{pmatrix} \qquad (11)$$

$$Q(\Omega, \omega, inc) = \begin{pmatrix} -cos(\Omega) \cdot sin(\omega) - sin(\Omega) \cdot cos(\omega) \cdot cos(inc) \\ -sin(\Omega) \cdot sin(\omega) + cos(\Omega) \cdot cos(\omega) \cdot cos(inc) \\ cos(\omega) \cdot sin(inc) \end{pmatrix} \qquad (12)$$

$$W(\Omega, inc) = \begin{pmatrix} sin(\Omega) \cdot sin(inc) \\ -cos(\Omega) \cdot sin(inc) \\ cos(inc) \end{pmatrix} \tag{13}$$

The transformation matrix T from the *PQW* frame to the *IJK* frame is simply

$$T(\Omega, \omega, inc) = [\, P \mid Q \mid W \,] \tag{14}$$

The positional vector p can be expressed in terms of the true anomaly ν as

$$p(\nu) = \frac{a \cdot \left(1 - ecc^2\right)}{1 + ecc \cdot cos(\nu)} \cdot (cos(\nu) \cdot P + sin(\nu) \cdot Q) \tag{15}$$

or alternately expressed in terms of eccentric anomaly E as suggested by Baluyev and Kholshevnikov[6] in their approach to determining minimum distance between two orbital paths

$$p(E) = a \cdot \left[(cos(E) - ecc) \cdot P + \sqrt{1 - ecc^2} \cdot sin(E) \cdot Q \right] \tag{16}$$

If a primary orbit (1) is not coplanar with a secondary orbit (2) then the vector of the line of mutual nodes J can be obtained from the angular momentum vectors of the two orbits

$$J = W\left(\Omega_2, inc_2\right) \times W\left(\Omega_1, inc_1\right) \tag{17}$$

$$J = \begin{pmatrix} cos\left(\Omega_1\right) \cdot cos\left(inc_2\right) \cdot sin\left(inc_1\right) - cos\left(\Omega_2\right) \cdot cos\left(inc_1\right) \cdot sin\left(inc_2\right) \\ sin\left(\Omega_1\right) \cdot cos\left(inc_2\right) \cdot sin\left(inc_1\right) - sin\left(\Omega_2\right) \cdot cos\left(inc_1\right) \cdot sin\left(inc_2\right) \\ sin\left(\Omega_1 - \Omega_2\right) \cdot sin\left(inc_1\right) \cdot sin\left(inc_2\right) \end{pmatrix} \tag{18}$$

The closest approach distance between the two elliptical, non-coplanar paths are not necessarily along this line of mutual nodes (Hoots et al[3]). It can, however, be used as a starting value for iteration to determine the minimum orbital intersection distance (MOID). For this work, it can also be used to begin a search to determine if the secondary orbit traverses the primary orbit's torus.

METHODOLOGY

Given primary (1) and secondary (2) Keplerian orbital elements, Equations 11-14 are used to express the components of the unit vectors of eccentricity (P), semi-latus rectum (Q), and orbital angular momentum (W) of the secondary orbit in the perifocal frame of the primary orbit.

$$\begin{pmatrix} P_x & Q_x & W_x \\ P_y & Q_y & W_y \\ P_z & Q_z & W_z \end{pmatrix} = T\left(\Omega_1, \omega_1, inc_1\right)^T \cdot T\left(\Omega_2, \omega_2, inc_2\right) \tag{18}$$

Using Equation 16 and the true anomaly ν_2 in this frame, the position vector of an object along the secondary orbit is

$$\begin{pmatrix} x \\ y \\ z \end{pmatrix} = \frac{a_2 \cdot \left[1 - \left(ecc_2\right)^2\right]}{1 + ecc_2 \cdot cos\left(v_2\right)} \cdot \begin{pmatrix} P_x & Q_x \\ P_y & Q_y \\ P_z & Q_z \end{pmatrix} \cdot \begin{pmatrix} cos\left(v_2\right) \\ sin\left(v_2\right) \end{pmatrix} \qquad (19)$$

If preferred, this vector can be found from the eccentric anomaly through Equation 16.

A secondary object with position (x, y, z) is on or inside the primary orbit's torus bounded by R_b and O_b if the following relationship from Equation 5 is satisfied.

$$\frac{\left[a_1 \cdot \left[\left(ecc_1\right)^2 - 1\right] + \sqrt{x^2 + y^2} + ecc_1 \cdot x\right]^2}{\left(\sqrt{x^2 + y^2} + ecc_1 \cdot x\right)^2} \cdot \frac{\left(x^2 + y^2\right)}{\left(R_b\right)^2} + \frac{z^2}{\left(O_b\right)^2} \le 1 \qquad (20)$$

Alternately, the object is on or inside the torus bounded by V_b and O_b if the following relationship from Equation 10 is satisfied.

$$\frac{\left[a_1 \cdot \left[\left(ecc_1\right)^2 - 1\right] + \sqrt{x^2 + y^2} + ecc_1 \cdot x\right]^2}{\left(\sqrt{x^2 + y^2} + ecc_1 \cdot x\right)^2 + \left(ecc_1\right)^2 \cdot y^2} \cdot \frac{\left(x^2 + y^2\right)}{\left(V_b\right)^2} + \frac{z^2}{\left(O_b\right)^2} \le 1 \qquad (21)$$

The three variables (x, y, z) in the above torus equations are all functions of only one variable, the true (or eccentric) anomaly of the second object. If no value for anomaly can be found on the interval $[0, 2\pi)$ to satisfy the appropriate torus equation, then the secondary orbit can be eliminated from further consideration because it won't intersect the torus. Regrettably, due to the transcendental nature of the torus equation, no analytical solution for anomaly exists.

NUMERICAL SEARCH

As previously mentioned, if the orbits are not coplanar then the vector of the line of mutual nodes J can be used to start a search to determine if the secondary orbit intersects the torus of the primary orbit. In this chosen frame

$$J = \begin{pmatrix} W_y \\ -W_x \\ 0 \end{pmatrix} \qquad (22)$$

The dot product of P and J is used to find the secondary orbit's true anomaly for nodal crossing

$$cos(v) = \frac{P_x \cdot W_y - P_y \cdot W_x}{\sqrt{\left(W_x\right)^2 + \left(W_y\right)^2}} \qquad (23)$$

The above has two possible solutions. At the node, the z component of Equation 15 must be zero. Therefore, the correct value of true anomaly is chosen to satisfy the equation

$$cos(v) \cdot P_z + sin(v) \cdot Q_z = 0 \qquad (24)$$

The antinode's true anomaly will be half a revolution from this node. Eccentric anomaly can easily be determined from these values if preferred. The nodal anomaly can then be used to start a search to determine if torus intersection can occur.

If $z^2 > O_b^2$ the torus equation cannot be satisfied. This condition can be used to bound the anomaly search by determining the limiting angles. In an approach similar to that taken by Woodburn and Dichmann[7], setting the z component of the secondary orbit to $\pm O_b$ in Equation 15 yields the expression

$$\pm Ob = \frac{a_2 \cdot \left[1 - \left(ecc_2\right)^2\right]}{1 + ecc_2 \cdot cos\left(v_2\right)} \cdot \left(cos\left(v_2\right) \cdot P_z + sin\left(v_2\right) \cdot Q_z\right) \tag{25}$$

The terms are rearranged to form

$$A \cdot sin(v) + B \cdot cos(v) = 1 \tag{26}$$

where

$$A = \frac{Q_z \cdot a_2 \cdot \left[1 - \left(ecc_2\right)^2\right]}{\pm O_b} \tag{27}$$

$$B = \frac{P_z \cdot a_2 \cdot \left[1 - \left(ecc_2\right)^2\right]}{\pm O_b} - ecc_2 \tag{28}$$

Using the intermediate angle δ, the following substitutions are made

$$C = \sqrt{A^2 + B^2} \tag{29}$$

$$A = C \cdot cos(\delta) \tag{30}$$

$$B = C \cdot sin(\delta) \tag{31}$$

into Equation 26 to produce

$$sin(\delta + v) = \frac{1}{C} \tag{32}$$

If C is less than one, then the secondary orbit never reaches the out-of-plane limit O_b. and no bounding anomalies exist. In this case, the two orbits are considered sufficiently coplanar that the entire range of anomaly $[0, 2\pi)$ must be searched to determine if the torus equation can be satisfied. Woodburn and Dichmann[7], using a simple distance function, suggested skipping the orbit path filter under this condition.

By comparing the z component to O_b through Equation 32, the limits of anomaly are found to be

$$\nu = \begin{pmatrix} asin\left(\dfrac{1}{C}\right) - \delta \\ \pi - \delta - asin\left(\dfrac{1}{C}\right) \end{pmatrix} \tag{33}$$

This pair of solutions is found for both possible signs of O_b to yield a total of four solutions, two for each nodal crossing. Any torus intersection that might exist must occur within these limits.

If it is determined that the second orbit cannot traverse the primary orbit's torus, then this pair can be eliminated from further analysis. This method uses simple two-body orbital dynamics which do not account for the changing geometry due to the precession of the orbital plane and the argument of perigee. It is therefore recommended[7] that this filter be employed throughout the time of interest at discrete intervals based on the distance settings and specific orbit characteristics. Conversely one can set the discrete time interval and then determine appropriate distance settings. These approaches are discussed in the sections that follow. If the second orbit cannot traverse the primary orbit's torus for all the interval times, only then should this pair be eliminated from further analysis.

PADDING

Filters such as this one are subject to false positive identifications (Type I errors) as well as false negative identifications (Type II errors). A Type I error occurs when the filter determines the satellite pair should be assessed further but no conjunction is then predicted. This is to be expected because the screening is based on the minimum distance between orbits. It will always be possible that the actual satellite positions will not come as close as their orbits, so Type I errors will occur because of the nature of the orbit path filter. A Type II error occurs when the filter determines the satellite pair should not be assessed further but a conjunction is then predicted. This reveals that the predicted satellite positions will come closer than the computed minimum distance between orbits.

Type II errors result from the simplifying assumptions that went into the path filter's development. One should add a pad or buffer to the desired distance threshold to reduce such errors and avoid missing possible conjunctions. Type II errors can be eliminated only with an excessively large distance pad which will, in turn, add a greater computational burden. A pad should account for the precession of the nodes and apsidal rotation as well as the secular and short-periodic variations for all the orbital elements (semi-major axis included). This pad should be chosen to strike a balance between timeliness and accuracy.

It is important for the user to configure the pad settings such that operational requirements are met in a timely fashion with an acceptable limit of Type II errors. This requires both step size control and distance bounds based on natural motion. Pad settings should be chosen in a manner that allows the end user to know whether the tool was exercised with a focus on accuracy or speed. If accuracy alone is important, one must be absolutely certain that the filter will not prematurely eliminate a pair of satellites from consideration that might be found to have a conjunction; Type II errors are not permitted. Such assurance comes with increased processing time as the computations would take much longer due to very conservative (large) pad settings. To absolutely assure no Type II errors, the simplest approach is to turn the orbit path filter off and assess every pair, accepting the increase in downstream computations. The padding strategies presented in the following test cases assume natural relative motion and should not be used if the ephemeris of either satellite contains maneuvers.

TEST CASE 1

To compare and contrast the torus- and distance-path filters, the entire Iridium constellation was screened for the day of April 19, 2010. This involved finding close approaches with all

objects in the public, TLE (Two Line Element), space catalog with a minimum range of less than 10 KM. The mid-day Keplerian mean elements were used by all filters. Tables 1a and 1b show the various pad settings as well as the number of pairs not eliminated by the Apogee/Perigee filter (Pairs Evaluated). The number of pairs eliminated by the orbit path filter (Pairs Eliminated) and Type II errors are included along with the total number of predicted conjunctions.

Table 1a. Test Case 1 for distance-path filter

Distance threshold (KM)	10	10	10
Apogee/Perigee Pad (KM)	30	30	30
Distance Pad (KM)	30	50	60
Pairs Evaluated	581759	581759	581759
Pairs Eliminated	479817	335898	226108
Conjunctions Predicted	714	1077	1260
Type II Errors	546	183	0

The numerical columns of Table 1a show the results of using a distance-path filter. For the case where the distance pad was set to 30 KM there were 546 Type II errors. Enlarging the pad to 50 KM yielded 183 Type II errors. Further enlargement of the pad to 60 KM yielded no Type II errors for the filter; when compared to the 30 KM distance pad case, however, the number of pairs to be evaluated downstream more than tripled.

Table 1b. Test Case 1 for torus-path filter

Distance threshold (KM)	10	10	10
Apogee/Perigee Pad (KM)	30	30	30
V_b Pad (KM)	30	30	50
O_b Pad (KM)	50	60	60
Pairs Evaluated	581759	581759	581759
Pairs Eliminated	390489	325991	254404
Conjunctions Predicted	1070	1258	1260
Type II Errors	190	2	0

The last numerical column of Table 1b reveals that the torus-path filter, with V_b and O_b pad values of 50 KM and 60 KM respectively, had no Type II errors. It also reduced the number of pairs to consider by 28,296 (over 12%) when compared to the 60 KM distance pad case in the last column of Table 1a. Comparing the previous Table 1b column (V_b pad set to 30 KM) to the 60 KM distance pad case, there are almost 100,000 less pairs to consider (over 44%) but two Type II errors appear. The first column, with V_b and O_b pad values of 30 KM and 50 KM, is included for comparison with the first two numerical columns of Table 1a.

The results for both types of filters can vary from day-to-day and the pads used here should be considered provisional for the Iridium constellation. As pointed out by Woodburn[4], the event detection logic needs to include a sampling strategy that accounts for important trends in the sampled metric. Several approaches involving pad-setting and sampling are presented in the following sections to address this.

TEST CASE 2

For this test, a large scale conjunction screening analysis was undertaken. This involved finding all conjunctions for 11,807 objects in the public TLE catalog with a minimum range of less than 10 KM for the seven day period beginning at 2009-02-10 16:00:00 UTC. Over 100,000 possible conjunctions were predicted with the path distance filter pad set to 30 KM and only employed once at the start of the scenario. This test case examines a resulting Type II error involving the premature elimination of a pair of satellites that would eventually come within 1.2 KM of each other. Table 2a provides the test case TLEs for this pair consisting of a SL-3 Rocket Body (NORAD ID 09904) and Fengyun 1C debris (NORAD ID 31921).

Table 2a. Test Case 2 TLEs

Object	Two Line Element Set
Primary	1 09904U 77024B 09041.51364740 +.00000011 +00000-0 -50667-6 0 05030
	2 09904 081.2589 194.8154 0053721 273.2500 086.2545 14.06530205634195
Secondary	1 31921U 99025CLY 09041.35799252 +.00000428 +00000-0 +49823-3 0 01655
	2 31921 099.3114 007.3534 0224626 349.6882 009.9561 13.64007839081997

For this analysis, Equation 21 is used to form the toroid distance function $f(v_2)$

$$f\left(v_2\right) = \frac{\left[a_1\cdot\left[\left(ecc_1\right)^2 - 1\right] + \sqrt{x^2 + y^2} + ecc_1\cdot x\right]^2}{\left(\sqrt{x^2 + y^2} + ecc_1\cdot x\right)^2 + \left(ecc_1\right)^2\cdot y^2}\cdot\frac{\left(x^2 + y^2\right)}{\left(V_b\right)^2} + \frac{z^2}{\left(O_b\right)^2} - 1 \qquad (34)$$

where x, y, and z are found from Equation 19 as functions of the secondary satellite's true anomaly v_2. It is valid for coplanar and non-coplanar orbits. For comparison with a distance-based orbit path filter, the values of V_b and O_b are both set to 40 KM (30 KM pad + 10 KM threshold). If the minimum value of f for all $[0^o \leq v_2 < 360^o]$ is positive then the secondary orbit never touches the primary orbit's toroid. If the value is zero, then the secondary orbit just touches the toroid surface. If the value is negative, then the secondary orbit pierces the toroid.
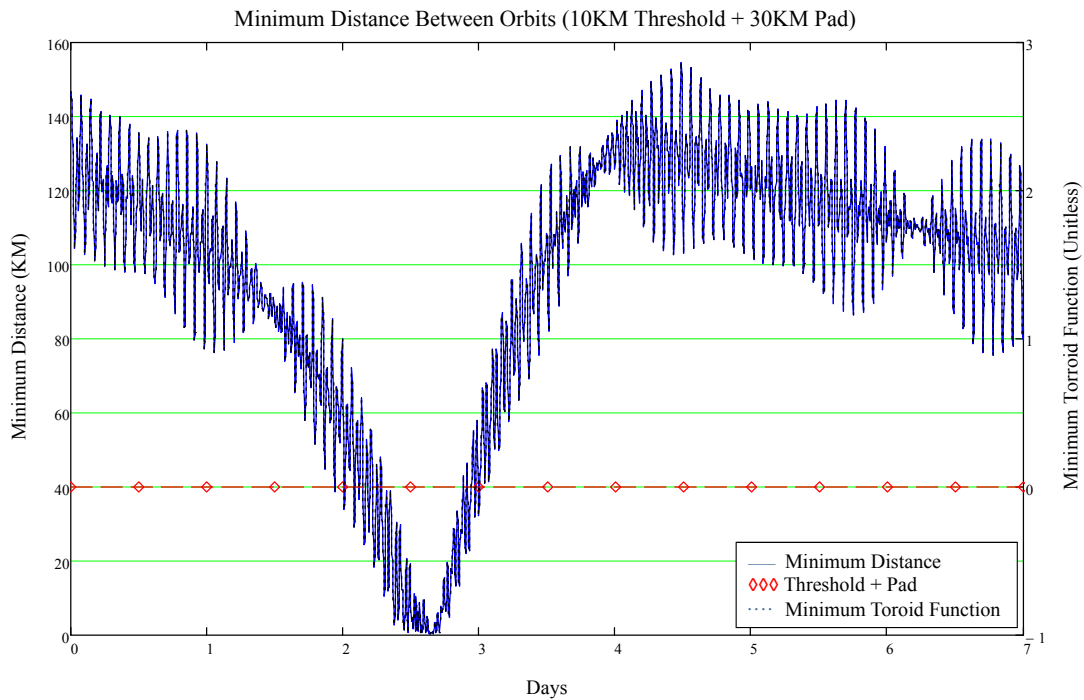
Figure 5. Miss Distance Between Orbits.

Figure 5 was created by propagating the TLEs in five minute increments to create ephemerides for both objects, determining the classical orbital elements for each instance of those ephemerides, and then determining the minimum distance between orbit paths. Such analysis is not limited to TLEs and will work with natural-motion ephemerides generated from any source. The left vertical axis of Figure 5 is the ordinate for the minimum Cartesian path-to-path distance between orbits (not satellite-to-satellite) over the seven day period. The right vertical axis is the ordinate for the minimum values of the toroid distance function *f*. As expected the two plots appear identical with only a difference in scale. The graph shows considerable frequency content and a wide range of variability over the seven day screening period. At scenario start (Day 0) the two orbit paths will not come within 100 KM of each other. Evaluating only this single data point, the orbit path filter would erroneously eliminate this pair from further consideration. Near Day 2.65 the orbit paths will come within 0.6 KM each other.

Minimum Distance Between Orbits (10KM Threshold + 30KM Pad)
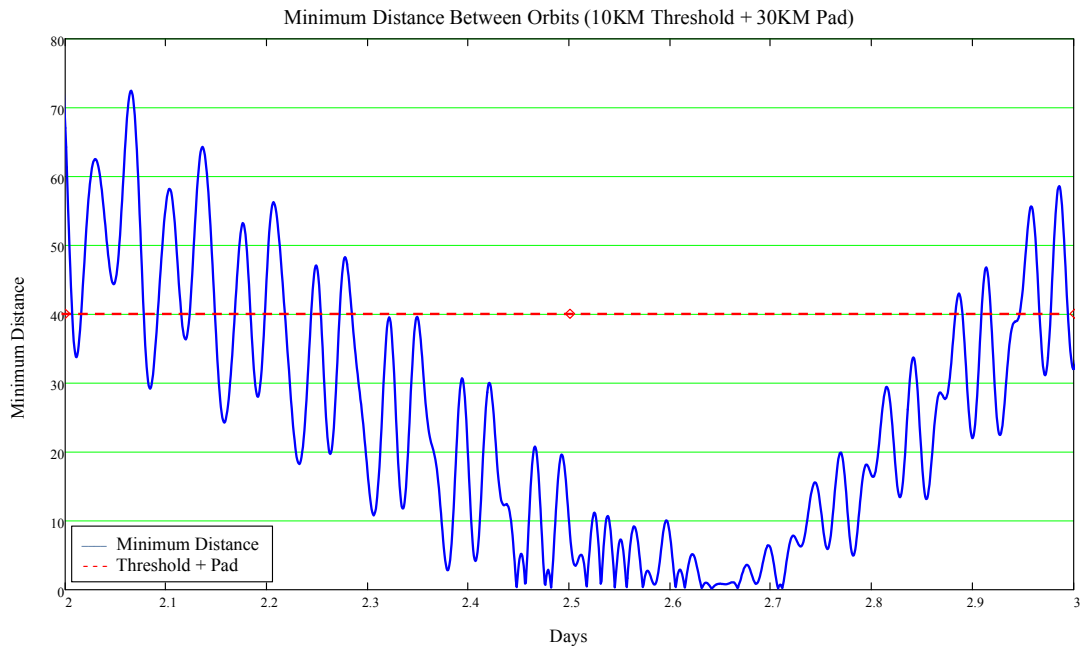
Figure 6. Minimum Time Interval to Assure Capture

Figure 6 focuses on the resulting orbit path behavior between Days 2 and 3, showing the time span that the minimum distance between orbits stays below 40 KM. For this specific case, the orbit path filter must be evaluated every 0.6 days or less to properly capture the minimum distance below the combined threshold (10 KM) and pad (30 KM). Returning to Figure 5, the diamond symbols show half-day sampling intervals. The orbit path filter would be evaluated each half-day until reaching Day 2.5, at which time the result would show the orbits coming sufficiently close to warrant further analysis.

A more complete approach to defining suitable pad limits is to determine the maximum path-to-path distance variability for a specific time interval within the period of concern. This goes beyond simply accounting for the differences between the mean and osculating orbit representations. Returning to Figure 5, one can plot the maximum variability to arrive at Figure 7. The time sampling intervals were examined in multiples of 2 hours, ending at half the scenario period.

Maximum Distance Variability (KM)
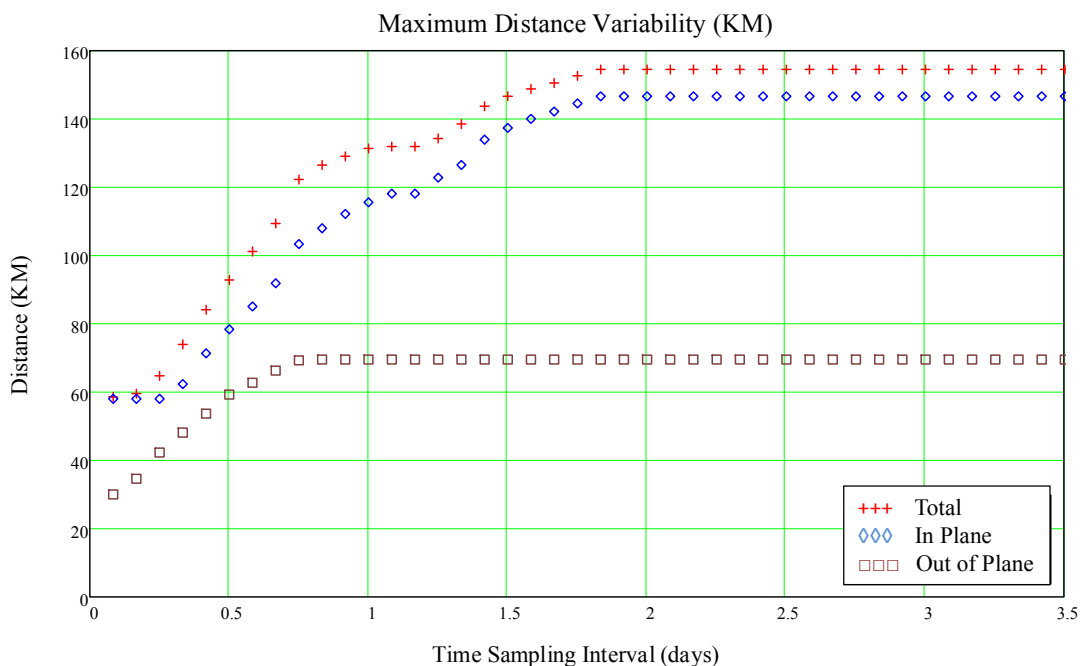
Figure 7. Time Sampling Interval versus Distance Variability

As Figure 7 illustrates for this satellite pair, an orbit path filter evaluation every 0.5 days would actually require a distance filter pad of 93 KM or in- and out-of-plane pads of 79 KM and 60 KM respectively. A larger pad or threshold allows a greater span and fewer orbit path filter evaluations. A time interval of one full day would require a total distance pad of 131 KM; two full days would require 155 KM. The larger pad would also identify more pairs for further consideration, many of which would be eliminated later in the process. Computational time would thus be reduced for filter evaluation but increased for further processing. Conversely, a smaller pad or threshold would require a smaller span and more filter evaluations. A time interval of four hours would only require a total distance pad of 60 KM. This would increase the computational time for filter evaluation but eliminate more pairs and reduce further processing time. For small time intervals the filter's computational burden may outweigh its benefit, meaning it might be faster to just assess the differences in satellite position and not use the path filter at all.

Settings of V_b = 89 KM (79 KM pad + 10 KM threshold) and O_b = 70 KM (60 KM pad + 10 KM threshold) with evaluation at the mid-time of each day are used to produce the last column of Table 2b. When compared to the 93 KM distance padded filter with the same evaluation times, the torus filter screened out 17% more pairs without introducing any Type II errors. The first numerical column of Table 2b simply shows the results of using a 30 KM distance pad.

Table 2b. Test Case 2 padding results

Distance threshold (KM)	10	10	10
Apogee/Perigee Pad (KM)	30	30	30
Distance Pad (KM)	30	93	NA
V_b Pad (KM)	NA	NA	79

O_b Pad (KM)	NA	NA	60
Pairs Evaluated	40883	40883	40883
Pairs Eliminated	33958	10725	12548
Conjunctions Predicted	160	185	185
Type II Errors	25	0	0

As with the previous test case, it must be emphasized that the pad sizes determined in this example are provisional. Many pairs must be assessed using the methodology used to create Figure 7 to assure no candidate pairs are erroneously eliminated by a pad size that is too small or a time sampling interval that is too big. This is demonstrated in the test case that follows.

TEST CASE 3

This case illustrates the conditional nature of the pad size by examining a case cited by Woodburn et al[4]. Table 3a provides the test case TLEs for this pair consisting of Thor Ablestar debris (NORAD ID 00130) and Delta 1 debris (NORAD ID 10730). Woodburn's team used a conjunction threshold of 5 KM for the seven day period beginning at 2009-02-12 05:00:00 UTC. These satellites come within 2.7 KM of each other within the first six hours of the scenario.

Table 3a. Test Case 3 TLEs

Object	Two Line Element Set
Primary	1 00130U 61015Q 09042.53163123 -.00000058 00000-0 13804-4 0 1891 2 00130 66.7709 101.1030 0080133 49.8006 311.0048 13.98086160426145
Secondary	1 10730U 75027E 09041.68856875 -.00000310 00000-0 -10589-3 0 6011 2 10730 114.9454 275.4040 0122342 287.9987 70.7850 13.92737619721619

Figure 9 was created using the previous test case methodology. Because no pad value was explicitly given in Reference 4, the 30 KM pad is again used with both V_b and O_b each set to 35 KM (30 KM pad + 5 KM threshold).
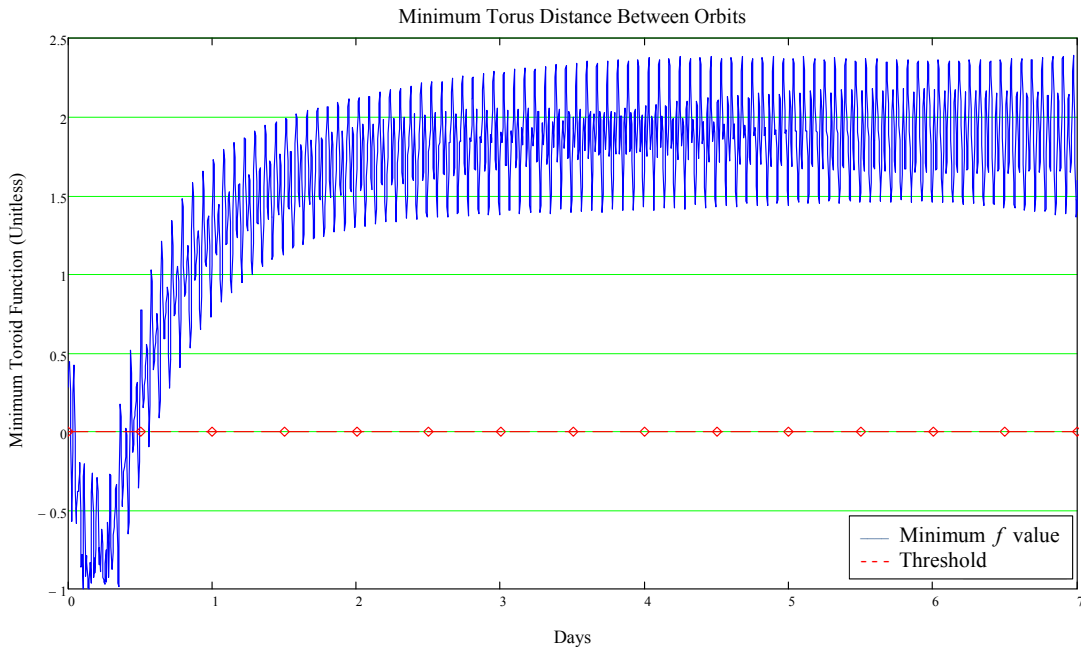
Figure 8. Toroid Function Values.

As can be seen in Figure 8, the pair would be eliminated if analysis was only done at the scenario start. With a very slight shift of scenario start time, however, even half-day incremental analysis would be insufficient to capture this pair for the pad setting of 30 KM.

Once again, suitable pad limits for this pair are determined by examining the maximum path-to-path distance variability for a specific time interval within the 7 day period of concern. Time sampling intervals of 2 hour multiples were used to produce Figure 9.
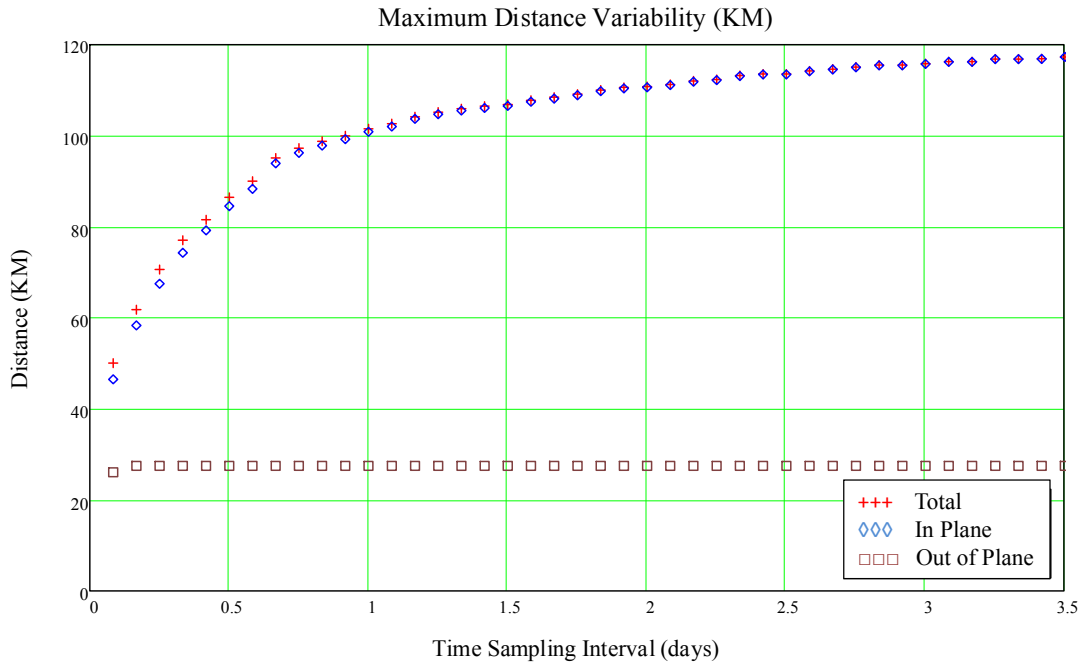
Figure 9. Time Sampling Interval versus Distance Variability

Based on Figure 9 and using a time sampling interval of 3.5 days, V_b is set to 123 KM (118 KM pad + 5 KM threshold) and O_b is set to 33 KM (28 KM pad + 5 KM threshold) to produce the third numerical column of Table 3b. When compared to the 30 KM distance padded filter with the same mid-span evaluation time, the torus filter screened out 3.4% fewer pairs and only eliminated one Type II error: the one associated with this specific conjunction. Comparison with the second numerical column using a distance pad of 118 KM shows that there are 11 other conjuncting satellites exceeding the torus' out-of-bounds pad, thus revealing the inadequacy of this pad size to eliminate all Type II errors. A sufficient number of pairs must be assessed for variability to assure completeness; this is an area of future research. As shown in the last column, increasing O_b to 60 KM eliminates all Type II errors while eliminating 38% more pairs than the distance-filter pad of 118 KM.

Table 3b. Test Case 3 padding results

Distance threshold (KM)	5	5	5	5
Apogee/Perigee Pad (KM)	30	30	30	30
Distance Pad (KM)	30	118	NA	NA
V_b Pad (KM)	NA	NA	118	118
O_b Pad (KM)	NA	NA	28	60
Pairs Evaluated	6428	6428	6428	6428
Pairs Eliminated	6191	1608	5980	2232
Conjunctions Predicted	4	16	5	16
Type II Errors	12	0	11	0

CONCLUSION

A toroidal approach to an orbit path filter was presented that provides more versatility than a simple distance function. This method uses the primary orbit to define a focus-centered elliptical ring torus with separate, user-defined, in-plane and out-of-plane bounds. An assessment is then made to determine if the secondary orbit can touch or penetrate this torus. After transformation to the primary satellite's perifocal coordinate system, the torus equation is derived as a function of only one variable, anomaly of the secondary orbit. The function is valid for coplanar, as well as non-coplanar, orbits. A numerical search method was presented due to the toroid function's transcendental nature. Three test cases were presented to compare and contrast the torus filter with a distance-only filter while also emphasizing the importance of properly choosing pad sizes. The test cases suggest that the torus filter can eliminate 10% or more candidate pairs than the distance-only filter without increasing Type II errors provided the pads are properly set. The padding strategies presented in the test cases assume natural relative motion and should not be used if the ephemeris of either satellite contains maneuvers. The results of these test cases can vary from day-to-day and should be considered provisional.

REFERENCES

[1] Kelso, T.S. and Alfano, S.: Satellite Orbital Conjunction Reports Assessing Threatening Encounters in Space (SOCRATES). 15th AAS/AIAA Space Flight Mechanics Conference, Copper Mountain, Colorado January 23-27, 2005, Paper AAS 05-124.

[2] Coppola, V.T., Dupont, S., Ring, K., Stoner, F.: Assessing Satellite Conjunctions for the Entire Space Catalog Using COTS Multi-core Processor Hardware. AAS/AIAA Astrodynamics Specialist Conference, Pittsburgh, Pennsylvania, August 9-13, 2009, Paper AAS 09-374.

[3] Hoots, F.R., Crawford, L.L., and Roehrich, R.L.: An analytical method to determine future close approaches between satellites. Celest. Mech. Dyn. Astron. 33, 143-158 (1984).

[4] Woodburn, J., Coppola, V., Stoner, F.: A Description of Filters for Minimizing the Time Required for Orbital Conjunction Computations., AAS/AIAA Astrodynamics Conference, Pittsburgh, Pennsylvania, August 2009, Paper AAS 09-372.

[5] Xue, D. and Li, J.: Collision criterion for two satellites on Keplerian orbits. Celest. Mech. Dyn. Astron. 108, 233-244 (2010).

[6] Baluyev, R.V., and Kholshevnikov, K.V.: Distance between two arbitrary unperturbed orbits. Celest. Mech. Dyn. Astron. 91, 287-300 (2005).

[7] Woodburn, J., and Dichmann, D.: Determination of Close Approaches for Constellations of Satellites., Paper No. C-5, IAF International Workshop on Mission Design and Implementation of Satellite Constellations, Toulouse, France, November 1997.